Investigation of precision grinding process for production of silicon diaphragms

A. Prochaska
S. J. N. Mitchell
Queen's University Belfast
School of Electrical and Electronic Engineering
Belfast BT9 5AH, United Kingdom

T. Perova
R. Maurice
University of Dublin
Trinity College
Department of Electronic and Electrical Engineering
Dublin 2, Ireland

P. T. Baine
H. S. Gamble
Queen's University Belfast
School of Electrical and Electronic Engineering
Belfast BT9 5AH, United Kingdom

Abstract. The application of precision grinding for the formation of a silicon diaphragm is investigated. The test structures involved 2–6 mm diam diaphragms with thicknesses in the range of 25–150 μm. When grinding is performed without supporting the diaphragm, bending occurs due to nonuniform removal of the silicon material over the diaphragm region. The magnitude of bending depends on the final thickness of the diaphragm. The results demonstrate that the use of a porous silicon support can significantly reduce the amount of bending, by a factor of up to 300 in the case of 50 μm thick diaphragms. The use of silicon on insulator (SOI) technology can also suppress or eliminate bending although this may be a less economical process. Stress measurements in the diaphragms were performed using x-ray and Raman spectroscopies. The results show stress of the order of 1×10^7–1×10^8 Pa in unsupported and supported by porous silicon diaphragms while SOI technology provides stress-free diaphragms. Results obtained from finite element method analysis to determine deterioration in the performance of a 6 mm diaphragm due to bending are presented. These results show a 10% reduction in performance for a 75 μm thick diaphragm with bending amplitude of 30 μm, but negligible reduction if the bending is reduced to <10 μm.
[DOI: 10.1117/1.1450597]

Subject terms: silicon grinding; silicon on insulator; porous silicon; finite element method analysis.

Paper JM3 001016 received Aug. 7, 2001; revised manuscript received Dec. 13, 2001; accepted for publication Dec. 21, 2001.

1 Introduction

The working principle of many microelectromechanical devices is based on the use of diaphragms as a flexural part, usually acting as a passive transducing element. The wide range of devices incorporating flexible diaphragms includes micromachined pressure sensors, microphones, and a variety of microfluidic devices such as micropumps and inkjet printheads.

The geometrical tolerance of the diaphragm during the fabrication process, as well as its thermal compatibility with the rest of the device, can have a significant impact on overall device performance. This is especially true in applications such as low-pressure sensing or precise picoliter liquid handling.

Different solutions have been employed in terms of materials and control of the geometry of the diaphragms. Pressure sensors years ago employed thin silicon diaphragms as the pressure sensitive element.[1,2] Diaphragms were formed by anisotropically etching exposed silicon areas, with the thickness of the diaphragms being controlled either by timed etching or by etch-stop techniques such as heavy boron doping or reverse $p-n$ junction formation. The flexural element in inkjet printheads and micropumps was usually made of stainless steel,[3] glass,[4,5] or silicon.[6,7]

The choice of diaphragm material is dependent on its compatibility with the overall fabrication process. In standard micromachining technology based on batch fabrication, the two main materials used are glass and silicon. Silicon is preferred since it offers a wider range of accurate micromachining processes and the possibility of integrating

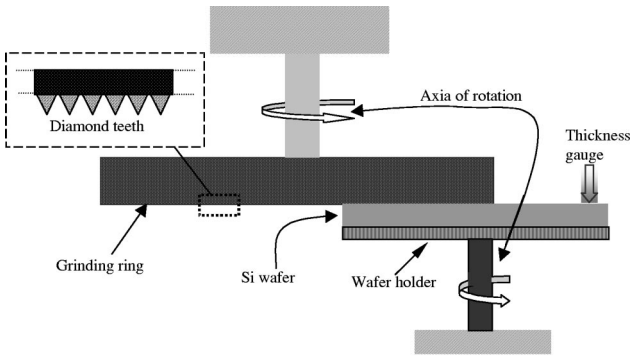

Fig. 1 Schematic cross section of the precision grinding system for silicon.

Address all correspondence to S.J.N. Mitchell, Tel: (4428) 90335437; Fax: (4428) 90667023; E-mail: n.mitchell@ee.qub.ac.uk

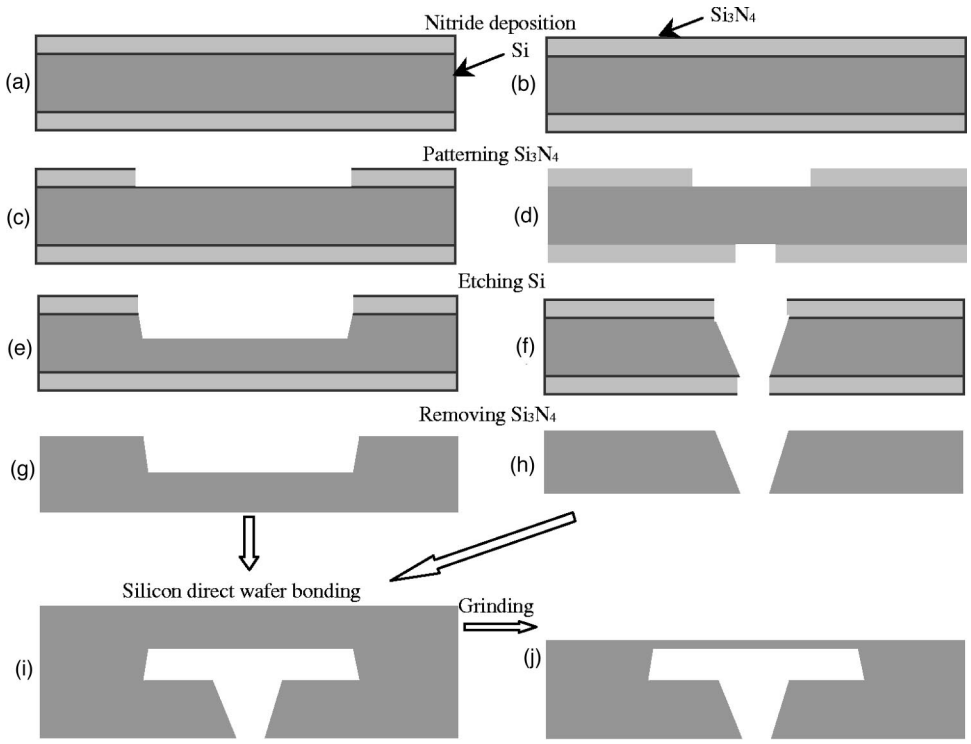

Fig. 2 Fabrication flow process for thin-diaphragm test structures.

electronic circuitry with microelectromechanical system (MEMS) structures.

In most cases silicon diaphragms are formed using etching, accompanied by etch-stop techniques. One alternative to this process is precise grinding of silicon, a technique that has been widely used in silicon on insulator (SOI) technology.[8] The main advantage of silicon grinding lies in its purely physical nature and time-saving efficiency. As an example, removal of 200 μm of silicon using anisotropic etching based on KOH aqueous solution in standard conditions takes 3–4 h whereas using grinding requires only 5 min. In the present paper we investigate the viability of precision grinding for the formation of silicon diaphragms.[9] Potential limitations of the process of diaphragm formation as well as techniques to overcome them are explained.

2 Silicon Precision Grinding

In this work a Shibayama VG-202MKII precision grinder was used. The system is capable of grinding 150 mm diam substrates with uniformity of ± 0.5 μm. A schematic cross section of the precision grinding of silicon is shown in Figure 1. The wafer holder may be slightly convex or concave in shape with a maximum convexity/concavity magnitude of 2–3 μm. The silicon wafer is held in place by vacuum.

The working mechanism is as follows: the grinding wheel and the silicon wafer are kept in direct contact while both are rotating. This causes constant removal of the silicon material as the result of friction between the diamond teeth and the silicon. A thickness gauge is used to determine the amount of material removed.

The process is purely physical and does not depend on parameters such as the temperature or wafer doping concentration. Precision grinding of silicon proceeds in two stages: coarse grinding followed by fine grinding. During the coarse grinding stage, the wafer and grind wheel rotate at 200–250 rpm, the removal rate of silicon is about 250 μm/min, and the wafer thickness tolerance is ± 3 μm. The fine grinding stage provides an improved wafer thickness tolerance of ± 0.5 μm at a slower removal rate of 20 μm/min. In applications in which an optically smooth silicon surface is required, an additional polishing step is necessary.

The most common use of the silicon grinding process is for the removal of a portion of the active wafer in the production of SOI substrates for MEMS and high performance electronic circuits.[8]

3 Fabrication of Test Structures

Two types of test structure were used in this work; those based on bonded wafer pairs or those on single silicon wafers. The minimum wafer thickness acceptable by the grinder used in this work was 250 μm. To ensure that this minimum is not exceeded and to preserve the overall strength and rigidity of test structures with thin diaphragms,

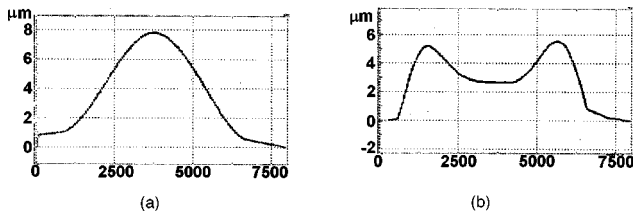

Fig. 3 Profile of (a) a 100 μm thick diaphragm and (b) a 25 μm thick concave diaphragm measured using the Alpha Step 200 (Tencor Instruments).

Table 1 Range of bending magnitudes within a wafer for each thickness of 6 mm diam diaphragms.

Wafer	A	B	C	D	E
Diaphragm thickness (μm)	~25	50	75	100	150
Bending magnitude range (μm)	Semiconcave	25.6–58.3	7.5–36.8	6–13.4	3.4–8.2

a process involving the bonding of two silicon wafers was developed. To prevent the bonding process from producing differential pressure on the diaphragm, a throughhole was etched into the support wafer. The preparation process for the bonded test structures is shown in Figure 2. Silicon wafers, 100 mm in diameter, with either *n*- or *p*-type doping were used. The initial thickness of the wafers was 525 ± 25 μm. The process starts with deposition of a 100 nm thick nitride layer on two wafers [Figures 2(a) and 2(b)]. Subsequently the nitride on the first wafer is dry etched to form 2–6 mm diam circular patterns [Figure 2(c)]. The second wafer is patterned with square openings and similarly etched [Figure 2(d)]. The next step consisted of KOH etching of the cavity [Figure 2(e)] in the first wafer and of the through holes in the second wafer [Figure 2(f)]. The depth of the cavity was within the range of 25–75 μm. After stripping the nitride from both wafers [Figures 2(g) and 2(h)], the wafers were bonded using a silicon direct bonding process in such a way that the opening in the second wafer was in the center of the cavity of the first wafer [Figure 2(i)]. The test structure was then ready for the precision grinding experiments [Figure 2(j)].

The above process was required to enable thin diaphragms <100 μm to be produced, however, for diaphragms >100 μm thick it was sufficient to use single wafers. In that case, 160 μm deep cavities were anisotropically etched into the front side of the wafer followed by grinding from the back of the wafer. The processing of single wafers is illustrated in Figures 2(a), 2(c), 2(e), and 2(g) followed by grinding. This process was used to form diaphragms 100 and 150 μm thick.

4 Results and Discussion

4.1 *Diaphragm Bending*

It was observed that the grinding process induced bending in the diaphragms. The magnitude of bending was measured using a surface-profiling instrument (Alpha Step). Bending occurred in the case of both bonded and single wafers, which precluded the bonding process from being the cause. The magnitude of bending depended on the thickness of the diaphragm and its location on the wafer. In all but one wafer the diaphragms had a convex shape and distortion magnitude, defined as the perpendicular distance between the top of the diaphragm and the wafer surface, and ranged between 3.4 and 60 μm for the diaphragm thickness between 150 and 25 μm, respectively. Diaphragms with a collapsed shape were observed on one of the wafers with a diaphragm thickness of 25 μm. Figures 3(a) and 3(b) show typical profiles of a 100 μm thick, 6 mm diam diaphragm and a ~25 μm thick semiconcave 6 mm diam diaphragm, respectively. For 6 mm diaphragms with thickness $\leqslant 50$ μm, most of the samples exhibited cracks after grinding.

The range of bending magnitudes within a wafer for a measured diaphragm thickness for 6 mm diam diaphragms are given in Table 1. The range of bending magnitudes for diaphragms 2–6 mm in diameter and 50 μm thick is given in Table 2.

4.2 *Bending Mechanism*

Two potential aspects of the grinding process and device structure that could cause bending stress were vacuum pressure acting on the bottom of the diaphragms and/or lack of a support for the diaphragms during the grinding process.

In order to investigate the first aspect, the back of the wafer was tightly sealed before grinding so that the vacuum did not affect the diaphragms. After grinding the bending still existed, indicating that vacuum was not the main cause of the bending.

In order to verify the second hypothesis the following experiment was implemented. Three plain wafers were thinned to 250 μm by precision grinding. Since no cavities were present, the underlying bulk silicon constantly and continuously supported the surface during the grinding process. After grinding, 6 mm diam cavities were etched according to steps (a), (c), (e), and (g) in Figure 2. The cavities in each wafer were etched to a different depth using KOH aqueous solution. The cavity depths were measured using the Alpha Step and the diaphragms were determined to be 25, 50, and 150 μm thick. After etching the cavities it was observed that, irrespective of their thickness, no bending of the diaphragms occurred. This reinforced the proposal that the bending was due to a lack of support for the diaphragms during the grinding process. Vacuum, however, may enhance diaphragm bending.

The forces that induce bending could have acted either parallel or perpendicular to the wafer surface or a combination of both. It was assumed that the distribution of those forces was symmetrical with respect to the center of the

Table 2 Range of bending magnitudes for 2–6 mm diam, 50 μm thick diaphragms.

Diaphragm diameter (mm)	6	4	3	2.5	2
Bending magnitude range (μm)	25.6–58.3	8.8–13.3	1.8–5.6	0.8–3.6	0.7–17

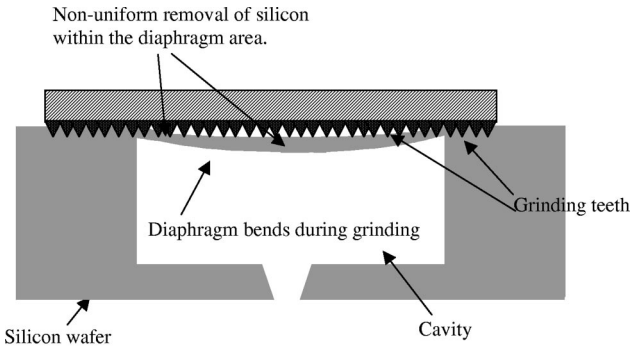

Fig. 4 Illustration of the mechanism of diaphragm bending formation during grinding.

diaphragms because of the bending symmetry.

If the forces that induce bending act in the plane perpendicular to the wafer, the bending magnitude w should be given by[10]

$$w \propto \frac{1}{h^4}, \tag{1}$$

where h is the diaphragm thickness.

Alternatively, if the forces act parallel to the wafer surface, then the bending magnitude w should be given by[10]

$$w \propto \frac{1}{h^2}. \tag{2}$$

In comparing bending magnitudes for diaphragms of different thicknesses, it was observed that in most cases the dependence followed Eq. (2) reasonably closely which suggests that bending stresses act in the plane of the wafer. Equation (2) would suggest that the bending ratio between 100 and 150 μm thick diaphragms would be 2.25. The experimental results were in good agreement with an average ratio of 2.13 (30 diaphragms were measured).

Forces parallel to the surface occur when there is a mismatch in the area of the top and bottom of the diaphragm caused by shrinking of one side or/and expansion of another. Such a mismatch is induced during the process of grinding by nonuniform removal of the silicon material in the diaphragm region because of the reduction in force exerted by the silicon on the grinding teeth. This is illustrated in Figure 4. Due to the increasing flexibility of the diaphragm and because of the lack of support underneath it, the diaphragm will deflect, with the largest deflection being at its center and the smallest near the edges. This in turn will cause nonuniform removal of the silicon material from the diaphragm (more material removed near the edges, less near the center) and as a consequence will induce a difference between the area of the top and bottom of the diaphragm and result in bending of the diaphragm.

5 Bending Prevention

The most straightforward way in which to prevent diaphragm bending is to grind the wafers before etching cavities and the formation of a diaphragm. This solution however applies only to the cases in which the total cavity and diaphragm thickness is large enough for the wafers to be handled as single ones. In cases in which the diaphragms are thin and/or it is necessary to perform silicon wafer bonding before grinding (see Figure 2), an easily removable support must be provided for the diaphragms. Two techniques, based on SOI technology and porous silicon, respectively, were investigated.

5.1 *SOI Technology*

SOI technology has been used to prevent diaphragm bending. The process steps are shown in Figure 5. Silicon dioxide, 0.2–0.3 μm thick, was grown on two batches of silicon wafers [Figures 5(a) and 5(b)]. Subsequently the wafers

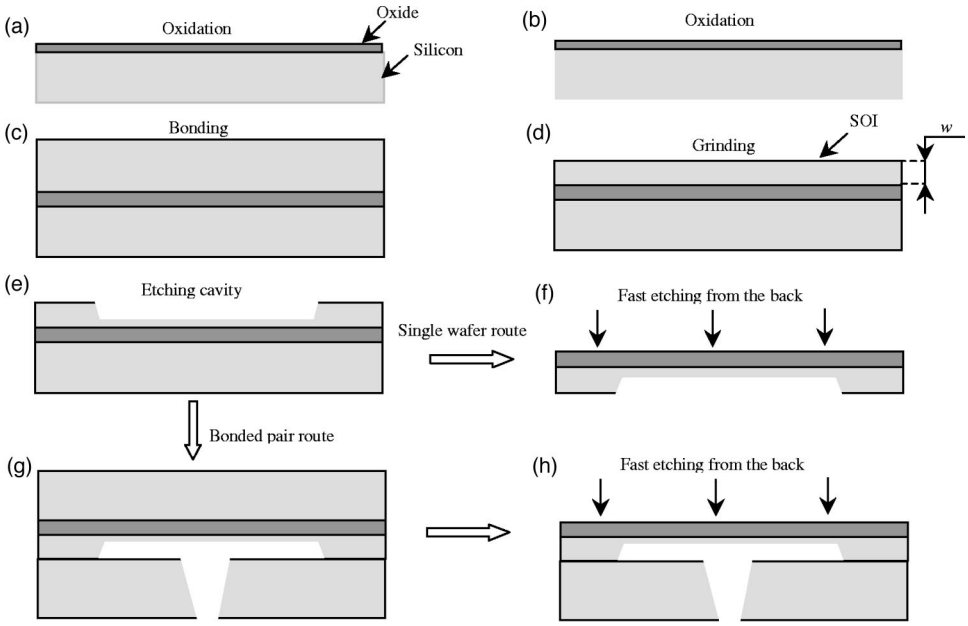

Fig. 5 SOI technology process for diaphragm bending prevention.

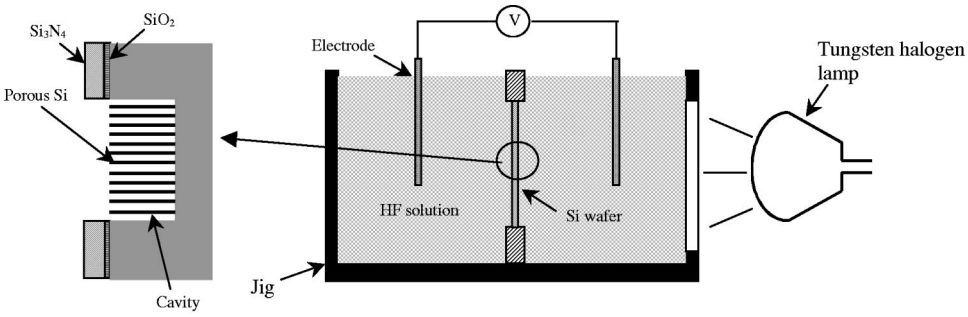

Fig. 6 Apparatus for porous silicon formation and schematic cross section of the cavity region of a silicon wafer.

were directly bonded [Figure 5(c)] and the oxide removed from the back of the wafers. Precision grinding [Figure 5(d)] was used to form a SOI layer of desired thickness, *w*, corresponding to the depth of the cavity and the thickness of the diaphragm. Cavities were etched into the SOI layer [Figure 5(e)]. For single wafer test structures, this was followed by etching from the back [Figure 5(f)] with the oxide acting as an etch-stop layer. If bonded structures are required, chemical mechanical polishing of the SOI is necessary to ensure a smooth surface at step (d). Following bonding [Figure 5(g)], the excess silicon would be removed by etching to give the structure shown in Figure 5(h).

No bending should occur, in either single or bonded wafer structures, because in both cases the diaphragm region is supported by silicon during the grinding steps.

An experiment was performed using the single wafer process on a 100 μm SOI layer with the cavities etched to a depth of 75 μm. Subsequently isotropic etching from the back of the wafer took place using 48% hydrofluoric acid:70% nitric acid:glacial acetic acid, 10:25:12 (HNA) solution to remove approximately 200 μm of the silicon followed by KOH etching until the oxide layer was reached. During the etching stages the front surface of the wafer was protected either by a special jig or by coating with wax. Even without removal of the oxide, no bending of the diaphragms was observed. Although employing the SOI method totally eliminates diaphragm bending it is not cost-effective because it requires an additional silicon wafer. A more cost-effective technique that employs the formation of porous silicon in the cavities before grinding was investigated.

5.2 *Porous Silicon*

A process that employs porous silicon was investigated to prevent diaphragm bending. The fabrication process started with the dry oxidation of two batches of silicon wafers to form a 6–15 nm thick protective oxide. Silicon nitride, 300–400 nm thick, was then deposited on both batches.

On batch 1, the front nitride and oxide was patterned to create a cavity window [see Figure 2(c)] and the back nitride/oxide removed by dry etching. Porous silicon was formed in the exposed silicon using an electrochemical reaction that converts the exposed bulk silicon into porous material. The nitride was subsequently removed using orthophosphoric acid.

Processing of the second batch followed steps (b), (d), (f), and (h) in Figure 2, and in step (h) the nitride was removed and the underlying oxide left in place.

Wafers from batch 1 were bonded to those from batch 2 using an aligned silicon direct bonding process. Precision grinding resulted in the formation of silicon diaphragms above the porous silicon regions. The final (optional) step is the removal of porous silicon from underneath the diaphragms; the high etch selectivity of porous silicon compared to that of bulk material means that this can be achieved with little effect on the diaphragms.

Porous silicon was formed using 1:1:2 HF:ethanol:water and 4:1 HF:ethanol solutions. The wafer was illuminated from the back using a 240 W tungsten–halogen lamp, shown in Figure 6. The current densities applied ranged from 4 to 9 mA/cm^2 and the depth of porous silicon ranged between 7 and 15 μm. After porous silicon formation and before bonding, the porous silicon was removed from some cavities by a short immersion in aqueous KOH solution (40

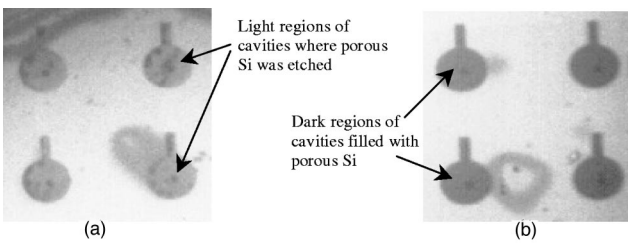

Fig. 7 Infrared images of parts of the bonded wafers with (a) porous silicon removed from the cavities before bonding and (b) cavities filled with porous silicon.

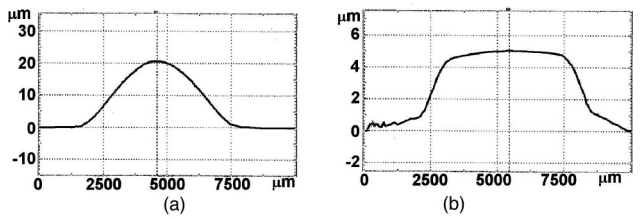

Fig. 8 Profiles of the diaphragms after grinding: (a) 75 μm thick without porous silicon and (b) $\leqslant$75 μm thick with porous silicon underneath.

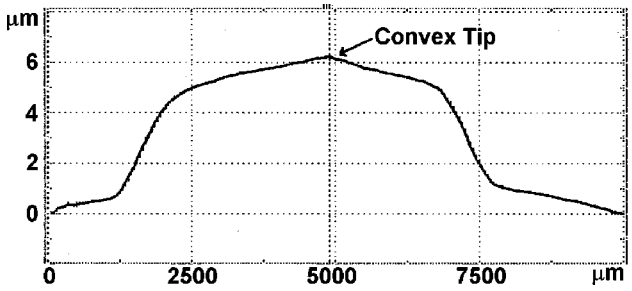

Fig. 9 Profile of a diaphragm with porous silicon support.

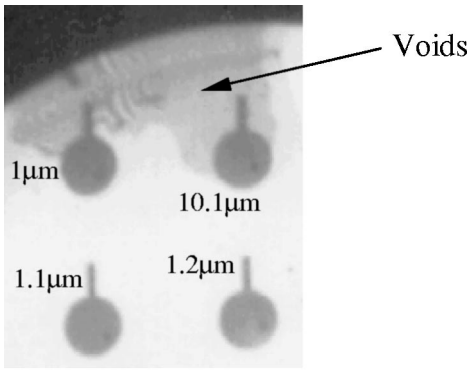

Fig. 10 Infrared image of the fully and partially bonded diaphragms with the diaphragm bending magnitude indicated.

wt. %). This allowed evaluation, within the same wafer, of the effect of porous silicon on diaphragm bending. Figure 7 shows infrared images of parts of a bonded wafer pair before grinding where four of the cavities are filled with porous silicon and the other four are not.

After the grinding stage and before removal of the porous silicon, the amplitude of bending was measured. It was observed that the presence of porous silicon during grinding strongly suppresses diaphragm bending. Figure 8 shows bending profiles of two 6 mm diam diaphragms. The first one [thickness 75 μm, Figure 8(a)] was formed without porous silicon and the second one [thickness $\leqslant$75 μm, Figure 8(b)] with porous silicon. It can clearly be seen that the use of a porous silicon support reduced the bending amplitude by a factor of 4, from $>$20 to 5 μm. The profile of the diaphragm is also noticeably different, with the unsupported diaphragm having a dome shape and the one that was supported being much flatter. It is believed that this is due to the porous silicon allowing some movement in the diaphragm during grinding but the movement is restricted when the porous silicon becomes compressed against the supporting wafer.

Some profiles of the diaphragms with porous silicon underneath showed a small tip at the center of the profile, like in Figure 9. The existence of the tip in the center of the diaphragm may be explained by the fact that in the center of the bottom of the cavities there are openings etched through the bottom wafer. During grinding there is less support provided for the area of porous silicon above the opening. Thus the area of the diaphragm above the opening will bend more during grinding than other parts of the diaphragm and lead to higher postgrinding distortion in that area. This is further confirmed by the fact that in samples in which the throughhole was toward one side of the cavity, no tip was noticed in the profile.

It was also observed that the diaphragm quality strongly depends on the bonding quality in the vicinity of the diaphragm's edge. Any voids resulting from bonding which come into contact with the cavity area usually cause a significant increase in the diaphragm postgrinding bending magnitude as illustrated in Figure 10.

The bending magnitude of the diaphragms supported by porous silicon depends mainly on two factors: the interfacial oxide thickness between the wafer surface and the nitride mask, and the structural properties of the porous silicon used. Figure 11 illustrates the dependence of the diaphragm bending magnitude on the two factors.[11] The presence of an interfacial oxide creates a gap between the surface of the porous silicon and the surface of the opposite wafer. During grinding this allows some deflection of the diaphragm and consequently postgrind bending of the diaphragm. Figure 11(a) shows that when the thickness of this interfacial oxide is reduced the diaphragm bending also becomes reduces. With no interfacial oxide, diaphragm bending is minimal. In comparison to unsupported diaphragms bending suppression was up to a factor of 300, demonstrating that use of porous silicon can virtually eliminate postgrinding diaphragm bending. Macroporous silicon with pore size 1–3 μm was found to be the most effective in suppressing diaphragm bending [Figure 11(b)]. Even dia-

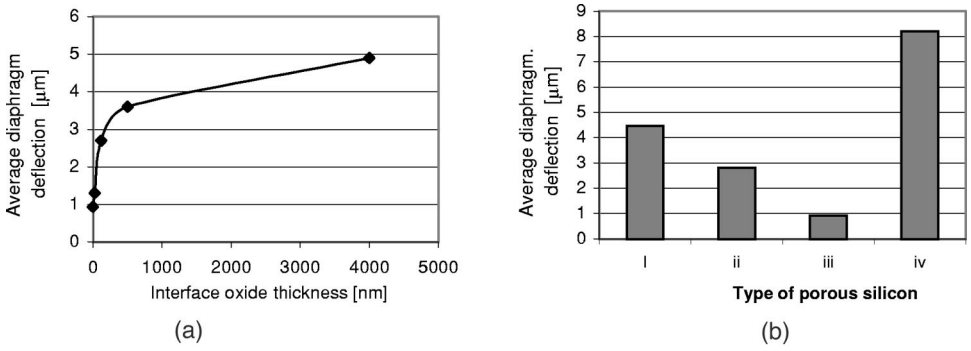

Fig. 11 Effect of (a) interface oxide thickness and (b) type of porous silicon on the diaphragm bending magnitude: (i) nanoporous, (ii) mesoporous, (iii) macroporous (pore size 1–3 μm), and (iv) macroporous (pore size 3 to over 10 μm), diaphragm thickness 50 μm (Ref. 11).

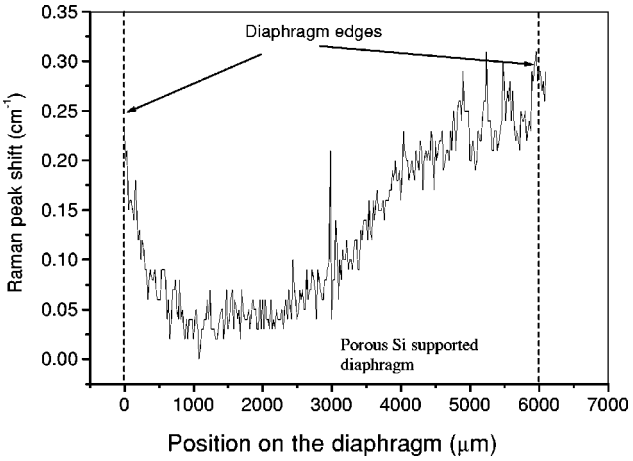

Fig. 12 Dependence of the shift of the Raman phonon line (at ~520 cm^{-1}) on the position on the diaphragm (the diaphragm edges are shown by the vertical lines) for a porous Si supported diaphragm after removal of porous Si. The positive shift corresponds to compressive stress, which varies from $\sim 1\times 10^7$ Pa at the center of the diaphragm to 1.4×10^8 Pa at the edges.

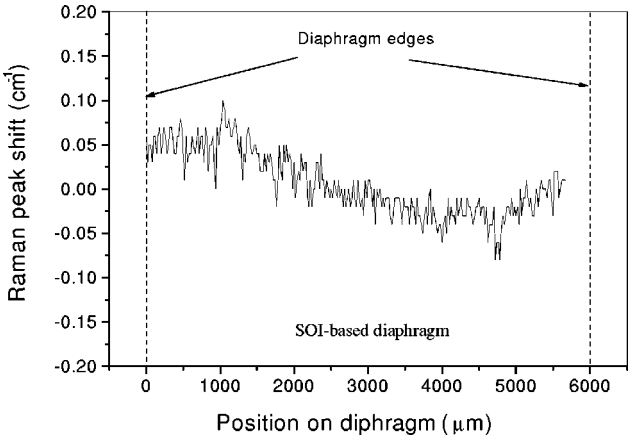

Fig. 13 Dependence of the shift of the Raman phonon line (at ~520 cm^{-1}) on the position on the diaphragm for a SOI based diaphragm. Virtually no stress is observed.

phragms with thickness 25 μm or less supported by porous silicon exhibited no cracks or damage after grinding.

6 Stress Measurements in the Diaphragms

Stress measurements in the both unsupported and supported diaphragms were performed using Raman and x-ray spectroscopies and the results are reported here in Sec. 6.

6.1 *Stress Measurements Using Raman Spectroscopy*

Raman spectroscopy has recently been successfully used for stress measurements in silicon.[12–17] Its main advantages are its nondestructive character, the simplicity of its setup, and the short time required for obtaining data.

In the present work Raman spectra were registered in backscattering geometry using a Renishaw 1000 micro-Raman system equipped with a Leica microscope and *XYZ* motorized stage. The use of a 100× magnification objective in the microscope and Ar ion laser with a 514 nm excitation line allows Raman imaging of the surface with spatial resolution of ~0.6 μm.

6.1.1 *Results and discussion*

The crystalline silicon Raman spectrum in a phonon region mainly consists of a narrow peak around 520 cm^{-1} with a half width of about 3.5 cm^{-1}. The spectrum is a result of scattering by long-wavelength transverse optical phonons.[12,13] With a state-of-the-art spectrometer it is possible to identify a shift in the Raman band of the order of ~0.01 cm^{-1}.[12] Removal of the background baseline followed by line fitting using a Lorentzian function allows three components of the Raman spectrum to be determined, namely, the intensity, the half width, and the position. These variations are related to the composition, defect density, and magnitude of stress, respectively. A relationship exists between the stress, σ, (in Pa) and the Raman shift, $\Delta\omega$ (in cm^{-1}):[12,15]

$$\Delta\omega = -2\times 10^{-9}\sigma, \tag{3}$$

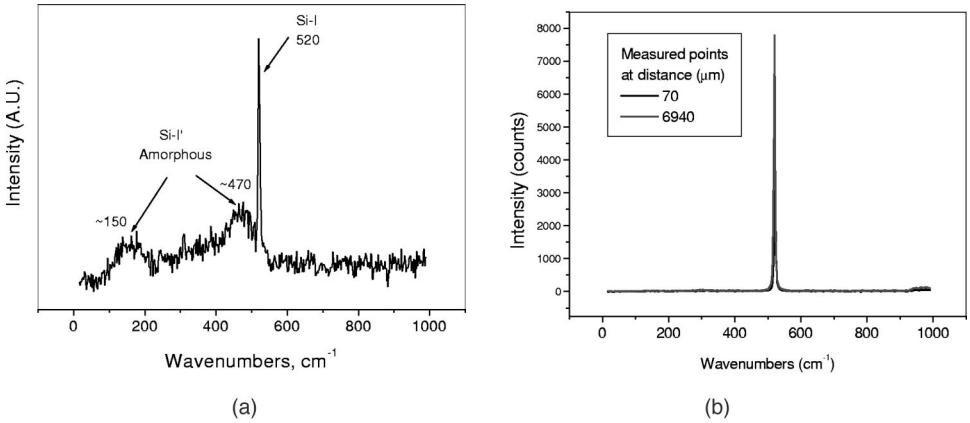

Fig. 14 Raman spectrum obtained (a) before and (b) after removal of the top surface layer after grinding.

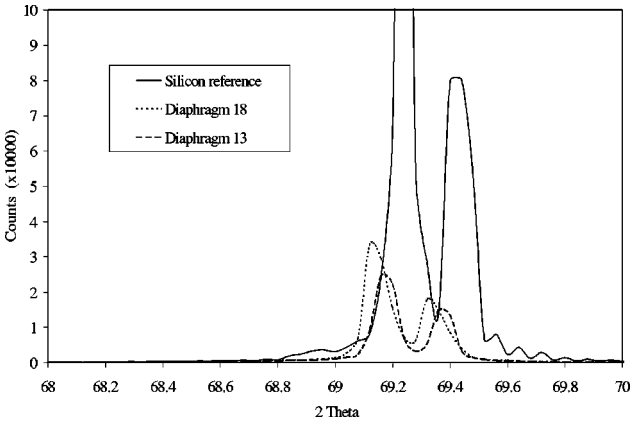

Fig. 15 X-ray stress analysis of the 100 μm thick diaphragms.

where $\Delta\omega=(\omega_{\text{stress}}-\omega_{\text{ref}})$ (in cm^{-1}), ω_{stress} is the peak frequency of the phonon band of silicon under stress, and ω_{ref} is the peak frequency of the phonon band of the stress free silicon wafer. A positive or negative shift in the Raman peak position corresponds to compressive or tensile stress, respectively,[12] assuming uniaxial stress only, i.e., within the plane of the wafer. Figure 12 shows the dependence of the shift of the Raman phonon line (at $\sim$520 cm^{-1}) on the position of the diaphragm which corresponds to distribution of stress across the diaphragm.

As one can see from Figure 12 porous silicon-supported diaphragms exhibit compressive stress that decreases from the edge of the diaphragm towards its center and similar results for unsupported diaphragms. For unsupported 50 μm diaphragms, stress was in the range of $0.5\times10^8-1.25\times10^8$ Pa, with most of the stress being relieved during diaphragm bending. For porous silicon-supported diaphragms stress was in the range of $0.75\times10^8-1.8\times10^8$ Pa before porous silicon removal and in the range of $1\times10^7-1.4\times10^8$ Pa after porous silicon removal. Raman spectra of the diaphragms based on SOI technology, shown in Figure 13, show virtually no stress, as expected (the deviations from 0 shown in Figure 13 are within the accuracy of the method).

Surface damage on the ground diaphragms was observed to consist of phase transformation into amorphous silicon, which is in agreement with that reported in Ref. 16. Figure 14 shows Raman spectra for, respectively, diaphragms after grinding and after subsequent removal of the top surface.

The spectrum in Figure 14(a) shows the existence of Si–I amorphous phase in the top ground layer. This phase disappears after the removal of the top several microns thick surface layer from the diaphragm and the spectrum shows silicon crystalline phase as illustrated in Figure 14(b).

6.1.2 *Stress measurements using X-ray spectroscopy*

Figure 15 illustrates the results obtained using x-ray spectroscopy. Three samples were analyzed: a plain silicon reference sample and two 100 μm thick bent diaphragms. The negative phase shift of the bent diaphragm samples with respect to the reference sample indicates compressive stress in the diaphragms, which is in agreement with the results obtained by Raman spectroscopy.

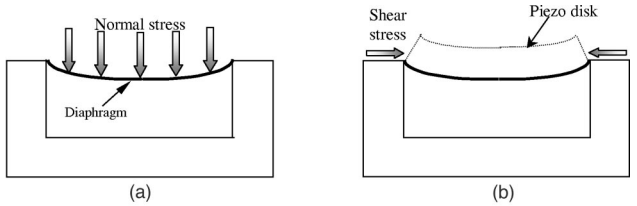

Fig. 16 Two basic actuation diaphragm modes: (a) normal and (b) shear stress.

7 Simulation

In order to evaluate the performance of the bent diaphragms, three-dimensional (3D) finite element method (FEM) analysis of the diaphragms was carried out using the CFD-FEMSTRESS package. The main emphasis was given to the deterioration in deflection of the bent diaphragms compared to that of an ideal flat diaphragm. The two most common diaphragm operating modes were simulated: normal stress mode and shear stress mode, shown in Figure 16. Normal stress is most commonly encountered in pressure sensors and in inkjet printheads that use stacked piezoelectric actuators. Shear stress mode occurs when a piezoelectric device is attached on top of the diaphragm due to lateral shrinkage during actuation. It was assumed in the simulations that the diaphragms have uniform thickness after grinding.

The simulated diaphragms were 75 and 50 μm thick. The graphs in Figure 17 show the percentage ratio between the deflection of bent diaphragms and that of a flat diaphragm of corresponding thickness. The same boundary conditions applied to all the diaphragms in respective simulation modes. The geometry of the diaphragms was taken from the Alpha Step profile by probing the profile at 8–10 points and subsequently applying interpolation. Residual built-in stress in the bent diaphragm was not taken into account in the simulation.

In comparing curves corresponding to normal and shear modes in Figure 17 it is seen that bending causes greater deterioration in the performance of the diaphragms when used in normal mode than when in shear mode. Also, for the same bending magnitude the performance deteriorates more with a decrease in diaphragm thickness. In the case of 75 μm thick diaphragms it is seen that for small distortions ($<$10 μm) performance deterioration in terms of deflection

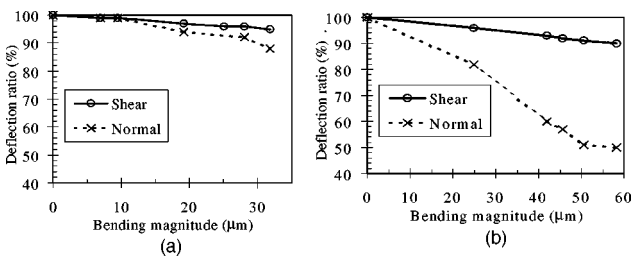

Fig. 17 Simulation of the deflection of bent diaphragms actuated in normal and shear modes for (a) 75 and (b) 50 μm thick diaphragms.

is marginal. The magnitudes of deflection in this range were observed in thick (>10 μm) diaphragms, which suggests that no support during grinding is needed in the case of thick diaphragms. In applications in which thinner diaphragms are required, the use of SOI technology or a porous silicon support layer has enabled diaphragm bending to be reduced to <10 μm at which it will have a minimal effect on diaphragm performance.

8 Conclusions

Precision grinding of silicon has been demonstrated for precise formation of silicon diaphragms. Diaphragms 2–6 mm in diameter and 25–150 μm thick were produced. It was observed that the process induces bending in the diaphragms if they are not supported during grinding. The use of SOI technology can virtually eliminate bending since the diaphragm is always supported by underlying silicon during the grinding steps, however, the process is less economical since an additional silicon wafer and a bonding step are required. The use of porous silicon as a support layer has been shown to significantly reduce the amplitude of bending by a factor of up to several hundred. Stress measurements of the diaphragms were performed using Raman and x-ray spectroscopies and indicate the existence of compressive stress of the order of $1\times10^{7}-1\times10^{8}$ Pa in unsupported diaphragms and in those supported by porous silicon, whereas the diaphragms based on SOI technology are stress free. Simulations of the bent diaphragms were performed using 3D FEM analysis. The results for 6 mm diam diaphragms indicate that deterioration of the performance, in terms of deflection, is negligible for diaphragms with convex bending of <10 μm.

Acknowledgments

The authors of this article would like to thank Randox Laboratories Ltd. for financial support and CFDRC Corp. for providing the CFD-FEMSTRESS tool.

References

1. Y. Kazui et al. ''Method for manufacturing diaphragm silicon pressure sensor,'' U.S. Patent No. 4,670,969 (1987).
2. Samaun, ''An integrated circuit piezoresistive pressure sensor for biomedical instrumentation,'' PhD thesis, Stanford University, Stanford, CA (1971).
3. E. Stemme and S. Larsson, ''The piezoelectric capillary injector: A new hydrodynamic method for dot pattern generation,'' *IEEE Trans. Electron Devices* **ED-20**(1), 14–19 (1973).
4. K. Petersen, ''Fabrication of an integrated, planar silicon ink-jet structure,'' *IEEE Trans. Electron Devices* **ED-26**(12), 1918–1920 (1979).
5. A. Olsson, P. Enoksson, G. Stemme, and E. Stemme, ''Micromachined flat-walled valveless diffuser pumps,'' *J. Microelectromech. Syst.* **6**(2), 161–166 (1997).
6. T. Laurell, L. Wallman, and J. Nilsson, ''Design and development of a silicon microfabricated flow-through dispenser for on-line picolitre sample handling,'' *J. Micromech. Microeng.* **9**, 369–376 (1999).
7. C. Meinhart and H. Zhang, ''The flow structure inside a microfabricated inkjet printhead,'' *J. Microelectromech. Syst.* **9**(1), 67–75 (2000).
8. K. Sadahiro, ''Method of manufacturing semiconductor substrate and method of manufacturing semiconductor devices composed of the substrate,'' European Patent No. 0460,437 (1991).
9. A. Prochaska, S. J. N. Mitchell, and H. S. Gamble ''Production of silicon diaphragms by precision grinding,'' U.K. Patent Application No. 0015500.2.
10. J. P. Den Hartog, *Advanced Strength of Materials*, McGraw–Hill, New York, (1952).
11. A. Prochaska, S. J. N. Mitchell, and H. S. Gamble, ''Porous silicon as a sacrificial layer during formation of silicon diaphragms by precision grinding,'' Proc. Int. MEMS Workshop, Singapore, pp. 743–747 (July 2001).
12. I. De Wolf, ''Micro-Raman spectroscopy to study local mechanical stress in silicon integrated circuits,'' *Semicond. Sci. Technol.* **11**(2), 139–54 (1996).
13. K. Ajito et al., ''Strain imaging analysis of Si using Raman microscopy,'' *J. Vac. Sci. Technol. A* **13**(3), 1234–1238 (1995).
14. S. Webster, D. N. Batchelder, and D. A. Smith, ''Submicron resolution measurement of stress in silicon by near-field Raman spectroscopy,'' *Appl. Phys. Lett.* **72**(12), 1478–1480 (1998).
15. Th. Englert, G. Abstreiter, and J. Pontchara, ''Determination of existing stress in silicon films on sapphire substrate using Raman spectroscopy,'' *Solid-State Electron.* **23**(1), 31–33 (1980).
16. Y. Gogotsi, C. Baek, and F. Kirsch, ''Raman microspectroscopy study of processing-induced phase transformations and residual stress in silicon,'' *Semicond. Sci. Technol.* **14**, 936–944 (1999).
17. I. Zarudi, and L. C. Zhang, ''Effect of ultraprecision grinding on the microstructural change in silicon monocrystals,'' *J. Mater. Process. Technol.* **84**, 149–158 (1998).

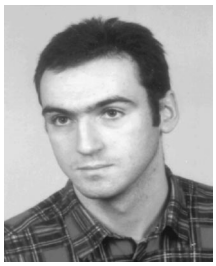

Andrew Prochaska obtained his MSc degree in 1997 from the Technical University of Lodz, Poland, and in 2001 was awarded a PhD degree in the area of Silicon Micromachining and Microtechnology from Queen's University Belfast, Northern Ireland (UK). His interests include solid-state MEMS technology. He is an author and coauthor of several international and national publications and holds one patent.

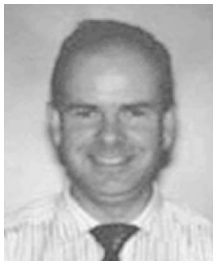

S. J. N. Mitchell received the BSc and PhD degrees in electrical and electronic engineering from the Queen's University of Belfast in 1982 and 1986, respectively. His research interests are in the development of semiconductor process technology and he has over 70 journal and conference papers published in this field. In recent years he has been involved in the development of bonding and silicon processing techniques for silicon micromachining applications. Particular emphasis has been on the development of technology for the fabrication of chemical microanalyzers and microfluidic devices.

Tatiana S. Perova received her MSc degree in Physics in 1969 from the Tajik State University at Dushanbe (Russia). She completed her PhD in Molecular Physics at Leningrad State University in 1979. Dr. Perova joined the staff of Vavilov State Optical Institute (St. Petersburg, Russia) in 1979, where she was involved in the characterization of condensed matter using far-infrared and Raman spectroscopies. In 1998 Dr. Perova took a position at the Department of Electronic and Electrical Engineering of the University of Dublin, Trinity College, where she has been involved in optical characterization of liquid crystals and thin films formed on silicon.

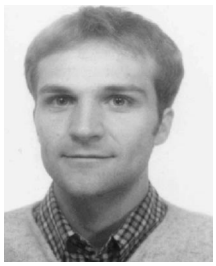

Remy N. Maurice has worked as a research assistant at the Department of Electronic and Electrical Engineering, University of Dublin, Trinity College, since February 2000. He has been involved in the phase transformation and stress analysis in silicon structures using micro-Raman spectroscopy. In 1999, he received his MSc in condensed matter from the University of Lyon, France, after he had completed the MSc degree at ISTIL, an engineering school, in Lyon, in 1998.

Paul Baine graduated with a BEng degree from Queen's University of Belfast. He went on to earn his PhD from Queens University in 1997. His PhD thesis dealt with the fabrication of thin single crystal silicon devices on glass using electrostatic bonding. After completion of his PhD, Paul took research posts at the university, expanding to the area of SOI where he has been involved in the development of novel techniques for the thinning of SOI material. He has also been involved in the bonding of nonstandard materials, including buried multilayer structures. Paul currently holds the post of Senior Microelectronics engineer at the Northern Ireland Semiconductor Research Center. His current research activities include SOI, MEMS, and materials science.

H. S. Gamble, a professor, has worked on silicon devices and related technology since 1966. He set up the first UK university polysilicon gate process for MOSTs in 1973 at Queen's University, Belfast, and submicron gate MOSTs were produced as early as 1981. He was the first to employ rapid thermal diffusion for the production of 250 nm deep boron junctions, which had the world's lowest leakage currents at the time. Bonded SOI substrates are of interest for bipolar and Smart-power applications. A unique SOI substrate suitable for MMIC applications was developed. CVD of metals is now being investigated for copper interconnects, barrier layers and for magnetic devices.